Available online at www.sciencedirect.com

SCIENCE DIRECT

Solid State Ionics 176 (2005) 905–909

SOLID STATE IONICS

www.elsevier.com/locate/ssi

A modified graphite anode with high initial efficiency and excellent cycle life expectation

Wang Guoping[a,b,*], Zhang Bolan[a], Yue Min[c], Xu Xiaoluo[c], Qu Meizheng[a], Yu Zuolong[a,c,*]

[a]Chengdu Institute of Organic Chemistry, Graduate School of Chinese Academy of Sciences, Chengdu 610041, China
[b]Department of Chemical Engineering, Central South University, Changsha 410083, China
[c]BTR Energy Materials Co., Ltd., Shenzhen 518036, China

Received 27 April 2004; received in revised form 13 November 2004; accepted 19 November 2004

Abstract

A new procedure was developed to prepare surface-modified graphite. First, spherical graphite (SG) particles were prepared through milling natural flake graphite (NFG). Then, surface-modified spherical graphite (MSG) was obtained by coating SG with a nanolayer of nongraphitic carbon. The SG exhibits better electrochemical performance than NFG, since there are significant decreases in the surface area and the probability of getting graphite basal planes parallel to the copper foil. It is also demonstrated that a nanolayer of nongraphitic carbon evenly covers the surface of SG. MSG with a core–shell structure shows higher initial coulombic efficiency and better cycle stability than SG because the carbon coating layer has improved its compatibility with electrolytes and protected the graphite against exfoliation.

Keywords: Lithium ion battery; Graphite electrode; Anode; Surface modification; Shape control

1. Introduction

After being introduced into the market as early as 1991, rechargeable Li ion batteries have become the key components of portable computing and telecommunication equipment required by an information-rich society. This is because they have the following advantages: high energy density, high operating voltage, good safety, and no memory effect [1–3] when compared with Ni–Cd or Ni–MH batteries. Although their advantages are prominent, investigation is still needed for reducing the thickness and weight of batteries and increasing their cycle stability. Therefore, the improvement of the anode material would advance the investigation one step further.

So far, the materials studied for lithium ion battery anode involve carbon materials, nitrides, tin oxides, and novel alloys [2,4]. Only carbon materials are commercialized, despite the great progress made by researchers with other anode candidates. The main reason for this is that Li ions can be intercalated into and deintercalated from the carbon materials reversibly. On the basis of their structure, carbon materials are categorized in three types: graphite or graphitic carbons, soft carbon, and hard carbon [5–8]. Among them, graphite or graphitic carbon materials, especially natural graphite, is considered to be one of the most important anode materials because it is superior to other carbon candidates in terms of high capacity, low irreversible capacity at the first cycle, flat and low potential profile, large amounts of resources, and low cost. Nevertheless, its disadvantages, such as its low volumetric density, high sensitivity to electrolytes, and easy exfoliation, are also remarkable. In order to overcome these disadvantages, vigorous investigation on the surface modification of graphite has begun.

Some authors [9,10] pointed out that coke-coated graphite exhibited some smaller irreversible capacity and better cyclability than pristine graphite. However, it decreased the total reversible capacity of the anode because coke showed lower capacity than graphite. Some metals [11,12], such as

* Corresponding author. Chengdu Institute of Organic Chemistry, Graduate School of Chinese Academy of Sciences, Chengdu 610041, China. Tel.: +86 288 522 3721; fax: +86 288 522 3978.
E-mail addresses: wgpcd@yahoo.com.cn (W. Guoping), yzuolong@mail.sc.cninfo.net (Y. Zuolong).

0167-2738/$ - see front matter © 2004 Elsevier B.V. All rights reserved.
doi:10.1016/j.ssi.2004.11.009

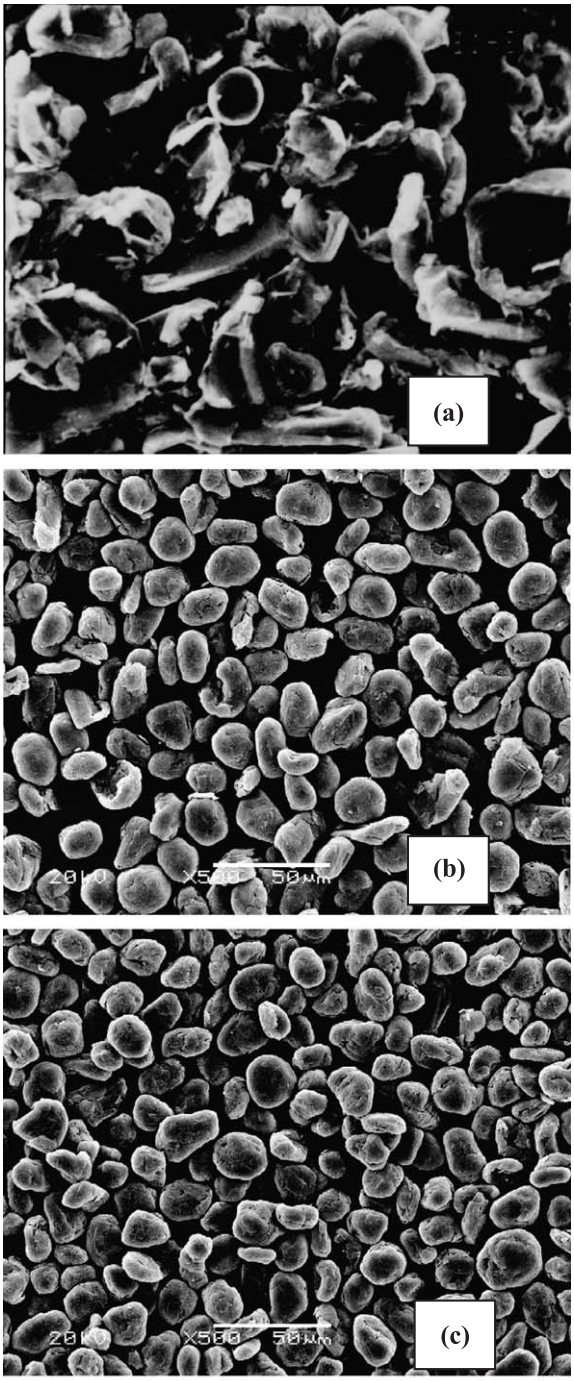

Fig. 1. SEM images of NFG (a), SG (b) and MSG (c).

Ag, Au, and Zn, were introduced onto the surface of graphite, too, and the rate capability and cycling behavior were improved. Obviously, these metals would decrease the power density of the graphite electrode due to their much higher atomic weight. In all of this literature, graphite without any pretreatment was directly coated with another kind of substance.

Presently, a new process for modified graphite is being developed. Natural flake graphite (NFG) was first milled to prepare spherical graphite (SG), which was then coated with a layer of nongraphitic carbon to prepare surface-modified spherical graphite (MSG) with a core–shell structure. Because the MSG holds quite a low surface area and probability of getting graphite basal planes parallel to the copper foil in the anode, the shell (nongraphitic carbon) protects the graphite core from exfoliation. Therefore, the MSG anode shows excellent electrochemical performance in comparison with NFG and SG, such as an initial reversible capacity of 365 mA h/g, which is close to the theoretical capacity of graphite, and a high initial coulombic efficiency of 93%.

2. Experimental

To prepare the SG sample, NFG was milled in a self-made miller for 12 h and then the milled graphite particles were sieved with a series of sizing devices. MSG was prepared as follows: SG was first dispersed in a solvent that contains the precursor of nongraphitic carbon and then the solvent was evaporated. Finally, the residue was treated at 900–1200 °C for 2 h under nitrogen atmosphere.

The average size of the carbon particles in the powders was measured with a Malvern laser diffraction analyzer. Surface areas of carbon particles were determined by nitrogen adsorption according to the BET method. The X-ray diffraction (XRD) patterns, which were obtained with a Philips PW1730 diffractometer using Cu Kα radiation, were utilized to analyze the crystal structure of graphite, and Raman spectroscopy was performed using an argon ion laser to analyze the surface structure.

The graphite composite electrode was fabricated as follows. First, 94% of active graphite, 3% of carbon black, and 3% of the binder LA132 were homogeneously mixed in an agate mortar and then the slurry was spread onto a 10-μm-thick copper foil to form an electrode. Next, the

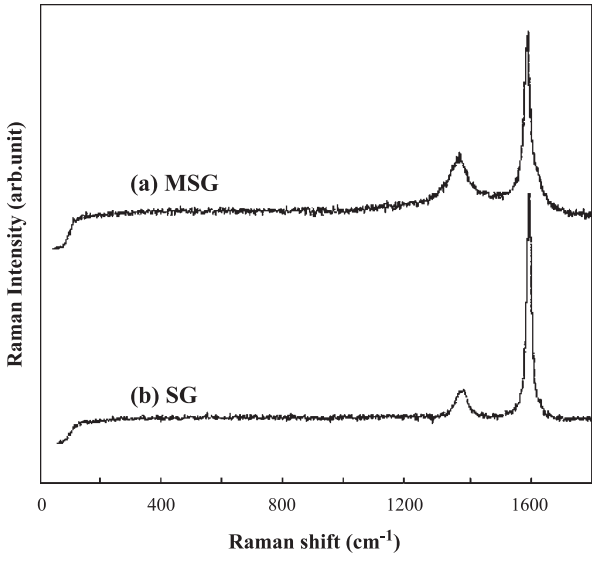

Fig. 2. Raman spectra of SG and MSG materials.

Table 1
Characteristics of the NFG, SG, and MSG materials

Sample	d(002) (nm)	Lc(002) (nm)	Content of 2H structure (wt.%)	Content of 3R structure (wt.%)	Surface area (m^2/g)	Volumetric density (g/cm^3)
NFG	0.3354	76.8	80.0	20.0	8.6	0.76
SG	0.3354	76.8	74.7	25.3	4.0	1.12
MSG	0.3368	76.8	82.5	17.5	1.2	1.36

electrode was dried under vacuum at 100 °C for 24 h, then pressed with a roller to enhance the contact of the particles. The electrode thickness was averaged 65 μm. The coin cells were assembled in a glove box under an argon atmosphere with a humidity rate of less than 5 ppm. A porous polypropylene separator (Celgard no. 2400) was packed into the cells.

The working electrodes were evaluated in a two-electrode cell in which a metallic Li sheet acted as the counter electrode. Electrochemical measurements of the charge–discharge of the graphite composite electrode were conducted in the electrolyte solvent EC/DMC (1/1 ratio in volume) containing 1 M LiPF6 (Mitsubishi Chemical) at room temperature. The cells were cycled between 2.0 and 0 V versus Li/Li^+.

3. Results and discussion

3.1. Characterization of the SG and MSG materials

Fig. 1a–c shows the typical SEM images of NFG, SG, and MSG, respectively. In Fig. 1b, the milled graphite particles are almost spherical and uniform in size. This observation confirms that SG can be obtained by milling.

Meanwhile, from Fig. 1b and c, it can be seen that the surface of the MSG particles appears smoother than that of the SG particles. This phenomenon points to the coating layer of nongraphitic carbon. The Raman spectra offer more convincing evidence for this.

It is well known that the laser Raman spectroscopy is effective in analyzing the crystallinity of carbon. In Raman spectra, two peaks, namely, the D-band at 1360 cm^{-1} and the G-band at 1580 cm^{-1}, could be assigned to nongraphitic and graphitic carbon, respectively. Fig. 2 shows the Raman spectra of the samples. The spectrum of SG exhibits a distinct G-band and a small D-band. With respect to MSG, the G-band becomes broader and smaller, and the D-band becomes broader and higher (Fig. 2b). The result is that the peak intensity ratio of the D-band and the G-band increases from 0.125 to 0.286. This clearly indicates that a layer of nongraphitic carbon evenly covers the surface of the graphite particles.

The mean diameters of the SG and MSG particles, in other words, D_0 and D_1, determined by a Malvern laser diffraction analyzer, are 19.711 and 20.497 μm, respectively. So, the thickness of the coating layer was calculated as 393 nm using the expression $(D_1-D_0)/2$.

According to XRD patterns, we know that all the samples of flake graphite have two kinds of crystal structure. One is hexagonal (2H), in which hexagonal planes are layered in a regular pattern in the order ABAB... The other is a rhombohedral (3R) crystal structure in which the planes are layered in the order ABCABC... In the process of the treatment described above, the structural carbon characteristics, such as the lattice spacing d(002), the relative content of the 2H and 3R crystal structures, and the size of the crystallite domains for the c-axis direction Lc(002), will change. To facilitate this comparison, Table 1 lists all of these characteristics obtained from XRD, their surface areas, and their volumetric densities.

The following conclusions are reached from Table 1.

- The MSG shows a larger lattice spacing d(002) than SG. The reason for this is that the coating layer classed as nongraphitic carbon has a lattice spacing 0.345 nm larger than that of graphite. The two peaks, which characterize nongraphitic carbon and graphite, respectively, overlap with each other in the XRD patterns and the result is that the 002 peak of MSG shifts in the direction of larger value in comparison with SG despite the small quantity of the coating layer.
- The fact that the content of 2H crystal structure decreases from 80% to 74.7% implies that the milling process has transformed part of the 2H crystal structure into 3R crystal structure. This is because the shearing force caused by milling is enough to make the basal planes, which are combined by van der Waals force, move. In contrast to the milling process, the heating process has translated part of the 3R crystal structure into 2H crystal structure.
- The surface area decreases in the order NFG, SG, and MSG, and the volumetric density decreases in the reverse order. Fig. 1 and the results shown in Table 1 indicate that

Table 2
Initial charge–discharge capacities and efficiencies of NFG, SG, and MSG anodes (D=discharge, C=charge)

Sample	1 M $LiPF_6$ EC/DMC=1:1			1 M $LiPF_6$ PC/EC/DMC=1/1/2		
	C capacity (mA h/g)	D capacity (mA h/g)	Efficiency (%)	C capacity (mA h/g)	D capacity (mA h/g)	Efficiency (%)
NFG	415	314	75.7	–	–	–
SG	403	360	89.3	–	–	–
MSG	390	366	93.8	406	366	90.2

the milling process has eliminated some edges and corners of graphite and improved its sphericity, and the coating layer has occupied part of the micropores and reduced structural defects in the graphite.

3.2. Electrochemical properties of the NFG, SG, and MSG anodes

Table 2 presents the initial charge–discharge capacities and efficiencies of NFG, SG, and MSG anodes in different electrolytes.

In Table 2, the active NFG material shows much higher initial irreversible capacity and lower reversible capacity than SG. The decreases in the surface area and structural defect can account for this phenomenon to some extent. To provide a more complete explanation, the shape of the particles should also be taken into account. As shown in the literature [13], in an NFG anode, we can observe that, due to their flake shape, the basal planes of graphite platelets are oriented horizontally (parallel to the current collector) while the basal planes of SG show a random orientation because SG is spherical (Fig. 3). Consequently, the diffusion resistance of Li ions in the SG anode falls and some more active materials are utilized in the process of charge/discharge. Hence, we can observe that SG exhibits better electrochemical performance than NFG. Table 2 also reveals that the MSG anode possesses some lower initial irreversible capacity and obviously higher initial efficiency than the SG anode. These are ascribed to the coating layer, which has further reduced the surface area of the graphite anode (Table 1), removed some active sites at the surface of naked graphite, and, therefore, reduced the irreversible side reactions leading to the formation of solid electrolyte interphase (SEI). The charge profiles of SG and MSG anodes shown in Fig. 4 also agree with Table 2. The SG anode shows an obvious plateau (at about 0.75 V) ascribed to the irreversible charge, whereas this plateau almost disappears for the MSG anode. In addition, it can be seen that MSG exhibits excellent compatibility with the electrolyte containing a PC solvent.

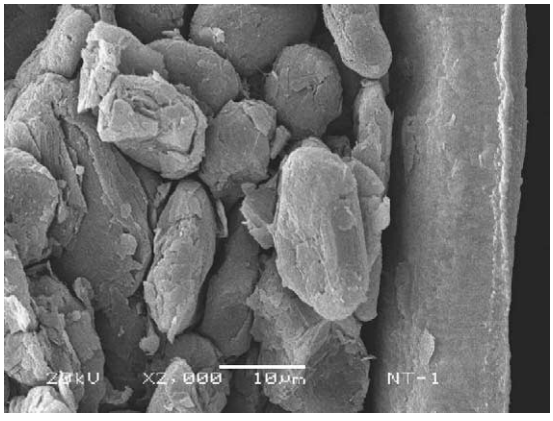

Fig. 3. SEM images of SG anode.

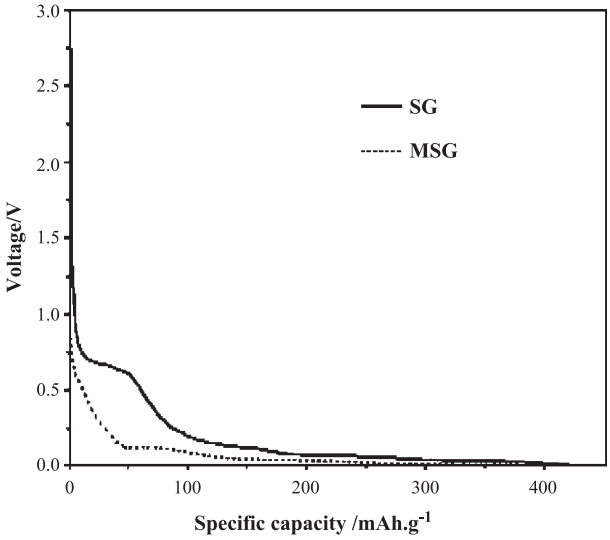

Fig. 4. Initial charge profiles of SG and MSG anodes.

With regard to NFG and SG, the charge/discharge could not be carried through in this case. This suggests that the coating layer considerably improves the compatibility of the graphite anode with the electrolyte.

Fig. 5 displays the cycling test results of the SG and MSG anodes in the electrolyte EC/DMC=1:1 (ratio in volume) containing 1 M LiPF6. For the active SG material, its retention ratio of reversible capacity dramatically decreases upon cycling. When it comes to the 100th cycle, the SG anode only holds about 60% of its initial capacity. While in the case of MSG, the anode still keeps 80% of its initial capacity even after 500 cycles. Without doubt, the coating layer of nongraphitic carbon contributes to the immeasurable contrast of cycle stability between the SG and MSG anodes. The roles of the coating layer can be summarized as follows: first, it has improved the compatibility of the anode with the electrolyte and prevented the solvent from cointercalation as well as irreversible losses during later cycles; secondly, it acts as

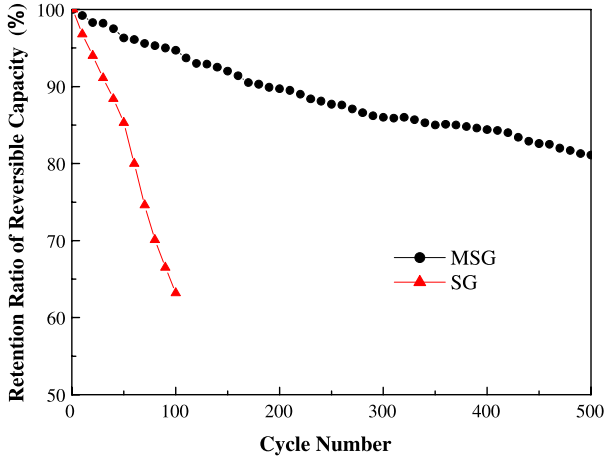

Fig. 5. Relationship between retention ratio of reversible capacity and cycle number.

an elastic film to protect the graphite core against exfoliation when the intercalation and deintercalation of Li^+ changes the volume of graphite during cycling.

4. Conclusions

SG particles can be well prepared through milling. The SG anode exhibits much better electrochemical performance than NFG, since there is a great decrease in the surface area, in structural defects, and in the probability of getting graphite basal planes parallel to the copper foil in the SG anode.

By coating SG with a layer of nongraphitic carbon, the as-prepared MSG with the core–shell structure shows higher initial coulombic efficiency and much better cycle stability than SG because the coating layer has improved the compatibility of the anode with the electrolyte, prevented the solvent from cointercalation, removed some active sites, and acted as an elastic film to protect the graphite core against exfoliation when the intercalation and deintercalation of Li^+ change the volume of graphite during cycling.

In conclusion, the graphite anode with higher initial coulombic efficiency and much better cycle stability could be prepared by means of the shape control of the graphite particle and surface modification.

References

[1] K. Zaghib, X. Song, A. Guerfi, R. Rioux, K. Kinoshita, J. Power Sources 119–121 (2003) 8.
[2] Y.P. Wu, C. Jiang, C. Wan, R. Holze, Electrochim. Acta 48 (2003) 867.
[3] D. Im, A. Manthiram, Solid State Ionics 159 (2003) 249.
[4] Y.P. Wu, E. Rahm, R. Holze, J. Power Sources 114 (2003) 228.
[5] H. Azuma, H. Imoto, S. Yamada, K. Sekai, J. Power Sources 81–82 (1999) 1.
[6] T. Kasuh, A. Mabuchi, K. Tokumitsu, H. Fujimoto, J. Power Sources 68 (1997) 99.
[7] I. Mochida, C. Hunku, S. Yoon, Y. Korai, J. Power Sources 75 (1998) 214.
[8] S. Ma, J. Li, X. Jing, F. Wang, Solid State Ionics 86–88 (1996) 911.
[9] S. Yoon, H. Kim, S.M. Oh, J. Power Sources 94 (2001) 68.
[10] K. Isao, Y. Masataka, J. Power Sources 54 (1995) 1.
[11] L. Shi, Q. Wang, H. Li, Z. Wang, X. Huang, L. Chen, J. Power Sources 102 (2001) 60.
[12] H. Momose, H. Honbo, S. Takcuchi, K. Nishimura, T. Horiba, Y. Muranaka, Y. Kozono, J. Power Sources 68 (1997) 208.
[13] D. Aurbach, M.D. Levi, E. Levi, A. Schechter, J. Phys. Chem., B 101 (1997) 2195.